

# Honey Badger Algorithm Using Partial Shading Condition MPPT Technique

<sup>1\*</sup>Arjun A., <sup>2</sup>Dr. P. Selvam

Submitted: 11/01/2024 Revised: 17/02/2024 Accepted: 25/02/2024

**Abstract:** The maximum production of electricity is needed to satisfy the consumption from sources of renewable energy, like solar power. The renewable energy source known as solar energy is also environmentally benign, making it an excellent option for power generation. Due to the fact that solar PV panel efficiency is dependent on irradiance, to optimize PV panel output, numerous methods for MPPT, or maximum power point tracking, has been created. Thus, a new method based on MPPT technique has been provided in this study to enhance the independent photovoltaic system's functionality even in dim lighting and climate change by using the algorithms HBA and COA. The HBA is extracted from the honey badger's method of foraging is employed to maximize the PV panel's power additionally COA optimization is analyzed for making the output power efficiently and accurately by analyzing the placement of PV panel in whole process based on the social behavior of coyotes. From these algorithms the maximum power is obtained in any climate changing situations and also the efficiency and accuracy are maintained using optimization. The novelty of this paper is to produce maximum power and also maintain the efficiency and accuracy of output throughout the process. Multiple simulation results are generated by the suggested algorithm, and the panel power is simulated using MATLAB software to assess its effectiveness. Comparing the suggested technique to the conventional algorithm at various degrees of solar brightness, the findings demonstrate that it can greatly increase regulated output power and provide faster, better dynamic response, hence increasing system efficiency.

**Keywords:** Partial shading condition, MPPT technique, PV system, Honey Badger Algorithm (HBA), Coyote Optimization Algorithm (COA), Efficiency, Accuracy.

## 1. Introduction

The growing population and advancements in technology are driving up the need for electricity, which is why power generation is shifting to more sustainable sources like solar energy. Solar energy is produced when sunlight strikes an object and is a cheap, infinite energy source [1]. The performances of the traditional P&O algorithm can be enhanced by applying the fractional short-circuit current (FSCC) approach in response to changing environmental circumstances [2]. Period of the next duty cycle that is used to enhance a photovoltaic system achieves its steady state by multiplying the adaptive perturbation size and variable perturbation frequency by an Arctangent function applied to a two-dimensional Gaussian function [3].

For low power and low cost applications, a significant voltage gain P&O technique has been implemented using an inverter-DC [4]. By looking at the algorithm for differential power, to effectively monitor the maximum

power, it ascertains boost converter's duty cycle, one may determine the difference between successive powers and related voltages [5]. To reduce oscillation with high speed and tracking accuracy is carried by fractional order with fuzzy logic method [6]. A variable step-size approach that auto-scales has been devised to eliminate the problems and to modify the step size using the previous variable step-size technique [7]. This paper focusing on the generating speed by increasing the number of optimal blades in which impeller solidity is measured using the starting and stopping speed of blades [8].

To improve PV system efficiency and reduce total harmonic distortion, a single phase multilevel inverter and three series-connected full bridge inverters are used in a single half bridge inverter configuration [9]. Its primary goal is to generate the most electricity possible under different shading condition in which whale optimization and differential evolution algorithms are used to produce high output [10]. This method is used to produce maximum power by reducing the shading effect and atmospheric changes using voltage scanning technique within the short period of complex PSC [11]. This system is made for low power applications that use photovoltaic systems with a single diode as the source of precision. System performance is improved by using the maximum power point tracking control approach [12]. To raise the renewable energy system's efficiency, the

<sup>1\*</sup>Ph.D. Scholar, Department of Electrical and Electronics Engineering, Vinayaka Mission's Kirupananda Variyar Engineering College, Vinayaka Mission's Research Foundation (Deemed To Be University), Salem-636308, Tamil Nadu, India.

<sup>2</sup>Professor, Department of Electrical and Electronics Engineering, Vinayaka Mission's Kirupananda Variyar Engineering College, Vinayaka Mission's Research Foundation (Deemed To Be University), Salem-636308, Tamil Nadu, India

<sup>1\*</sup>Corresponding Author Email: arrjun011@gmail.com

P&Q algorithm monitors the input source's maximum power point. The temperature affects a solar system's output power and radiation intensity of the solar cells [13]. This system uses an array of PV cells with the MPPT algorithm of fuzzy mechanism and deep reinforcement to continuously create the maximum power [14].

This research aims to enhance photovoltaic panels using algorithm for producing maximum power and by algorithm but in conventional technologies the maximum power is not stable to all type of loads. The remaining portions of this work are separated into the following categories. The investigated PV panel model is explained in Section 2. Section 3 describes the architecture of the boost type dc-dc converter. In section 4 offers a thorough assessment of the MPPT tracker's performance utilizing a closed loop PID controller and the suggested algorithm in separate sections. Section 6 concludes with a conclusion. Section 5 displays the experimental validation together with the findings of the simulation.

## 2. Literature Review

DC to DC converters are used with MPPT algorithm to produce maximum power; however these types of converters are used with MPPT algorithm only in PV system. In this section some existing papers related to this technology are reviewed.

A DC – DC converter based on the PV fed solar PV system for low power applications was discussed in this system. For the same PV system, the same people were the focus of the creation and modeling of a single diode-based solar panel. The system will operate more accurately if the solar panel receives less irradiation. Maximum Power Point Tracking (MPPT) control algorithm, which was examined by Akhil Raj et al. [15], is employed with the same system to improve performance. Furthermore, a comprehensive investigation on DC-DC converters with a flexible switching mechanism and a solar-fed system is underway.

In this technology, M. Lakshmi et al. provide a single-phase DC-DC high-gain converter as a solution to the dual utilization of DC to DC converter in PV systems connected to the grid [16]. One key benefit of this converter for achieving integrated MPPT control and DC voltage regulation was its ability to operate three switches in two separate modes. Even when the inverter is not connected to the DC bus, this integrated control aids in maintaining a consistent DC voltage for the DC load.

To monitor maximum power point (MPP) modules for photovoltaic performance, fill the greatest amount of energy output available, and maintain reliability and

efficiency, several tracking methods are investigated. Khaled Osmani et al. employed two phases in this system: the DC-DC Power Processing Unit (PPU) architecture and algorithm implementation [17]. Initially, low & partial irradiance conditions are the design parameter for all MPP algorithms. Second, PPU's were categorized as DC-DC converters that were either independent or non-isolated. When creating an MPP tracker, a separate buck-boost converter is the optimal option, according to PPU design.

A PV-powered water pump system with a quadratic Boost (3LQB) and a flexible suspension drive (SRM) with three stages of DC-DC dual conversion was unveiled. The attainment of quadratic static voltage, the DC-DC topology was distinguished by a drop in electrical pressure across all power switches and diodes and power to maintain electrical balance in the output capacitors. An asymmetrical half-bridge (AHB) converter attached to the SRM drive is turned on by the DC-DC converter's three-level voltage. Additionally, the DC-DC converter's continuous running mode (CCM) optimizes power produced by photovoltaic cells when combined with the high-performance tracking algorithm (MPPT) developed by Armando Cordeiro et al. [18].

This approach is used to construct and examine a solar system that is managed by a Fractional Order PI (FOPI) controller and has a strong DC-DC Transistor. Strengthening the DC-DC converter is required in order to track inputs effectively. Goal of Ahmed T. Mohamed et al.'s study [19] was to determine the appropriate PV model's parameters and FOPI controller's operational settings. Using flower pollination algorithm (FPA) and water cycle algorithm (WCA), the features of the PV module models and the FOPI control panel were specifically specified.

MPPT was implemented in three phases with a fixed and flexible step of current interference to improve its durability and performance which was presented by S.M.Sousa *et al.* [20]. This MPPT algorithm was tested by testing three separate DC converter heads controlled by a single loop of current for testing feasibility of this system in sudden change of irradiance, which was used in off-grid photovoltaic battery charging systems.

## 3. Design Of Proposed Methodology

The PV has been examined and assessed in this suggested technique. By implementing the analyses, it has been confirmed that the suggested method for analyzing the PV system is effective. Determining the PV system's metrics, such as its efficiency and losses, the suggested method is used. Present in the PV system are three categories of analysis: technical sustainability, viability, and verifying and defending environmental

conditions. The recommended solution consists of a controller, DC-AC inverter, PV panel, and switched mode DC-DC transistor. In addition to assessing accuracy and efficiency, the highest power is extracted using this method. Figure 1 displays the PV units' block diagram in its entirety of this paper in this PV panel accept the irradiance of sunlight which is integrated with MPPT block for getting maximum power this maximum power. With the aid of an inverter, this maximum power is transformed from DC to AC to supply loads [21].

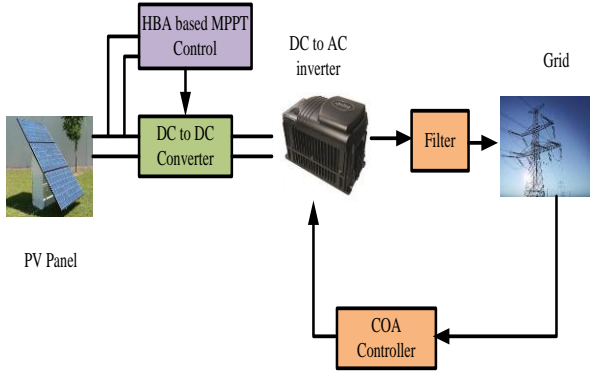


**Fig 1:** The block diagram of solar power system

To achieve maximum power, using HBA based MPPT algorithm. Each and every block of this system is explained in below sections.

#### 4. Output Voltage and Current Analysis Of PV Panel

Solar panel which combines several PV cells to provide high power is the initial component of the suggested system that is utilized to transform light energy into electricity. A photovoltaic cell, also known as a PN junction diode, is composed of semiconductor materials with positive and negative layers that contain holes and electrons, two types of charge carriers. Figure 2 displays the PN junction diode circuit schematic. Since no solar cell is really suitable for employed as a current source in conjunction with a diode, the model has a component for both series resistance and shunt resistance [22].

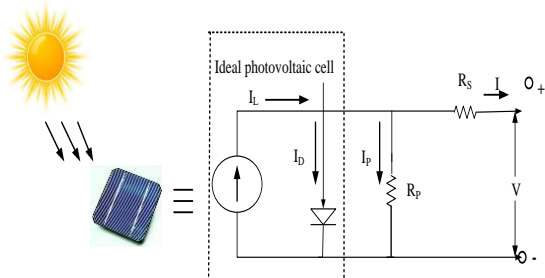


**Fig 2:** Circuit diagram of PV cell

Solar cell's current production is mentioned in equation (1) that is equal to the addition of diode current and current through the shunt resistor is subtracted from that produced current source.

$$I = I_L - (I_D + I_p) \quad (1)$$

Here, the output current is represented by  $I$ , the photo current by  $I_L$ , the diode current by  $I_D$  and the shunt current is denoted as  $I_p$ . Voltage across these elements determines the current flowing through them, as stated in equation (2)

$$V_j = V + IR_s \quad (2)$$

Where  $V$  is the voltage across the output terminal and  $V_j$  is the voltage across the diode and resistor, output current is denoted as  $I$  and series resistor is denoted by  $R_s$

Equation (3) mentions the diode current, which comes from the Shockley diode formula.

$$I_D = I_o \left\{ \exp \left[ \frac{qV_j}{nKT} \right] - 1 \right\} \quad (3)$$

Where, the symbols for elementary charge are represented by  $q$ , diode ideal factor by  $n$ , reverse saturation current by  $I_o$ , Boltzmann's constant by  $K$ , and absolute temperature by  $T$ . At  $25^\circ\text{C}$ ,  $\frac{KT}{q} = 0.0259$

volts. Current passing through shunt resistor can be calculated using formula (4).

$$I_p = \frac{V_j}{R_p} \quad (4)$$

Here,  $R_p$  is the shunt resistance. Substituting these values in equation (1) we obtain the output current and voltage, which are provided by equation (5).

$$I = I_L - I_o \left\{ \exp \left[ \frac{q(V + IR_s)}{nKT} \right] - 1 \right\} - \frac{V + IR_s}{R_p} \quad (5)$$

To find the value of  $V$ , Lambert's W function is used to solve the equation.

At  $I = 0$  (open circuit), the voltage across the output terminals equals the open-circuit voltage of the cell. When the shunt resistance is large enough, the characteristic equation's last factor is ignored, the open-circuit voltage  $V_{oc}$  is mentioned in equation (6).

$$V_{oc} \approx \frac{KT}{q} \ln \left( \frac{I_L}{I_o} + 1 \right) \quad (6)$$

The short-circuit current,  $V = 0$ , is defined by equation (7) as the current that flows through the terminals while the cell is functioning in a short circuit.

$$I_{sc} = I_L \quad (7)$$

As a result, the levels of voltage and current produced by solar cells are calculated using the previously given formula. After that, the DC to DC converter block—which is shown in the block below—receives these voltages.

#### 4.1. Performance and circuit diagram of DC to DC converter

DC-DC converter block uses PV panel's output voltage as its input to raise the input voltage to a predetermined level. In this instance, a boost type DC-DC converter is utilized; figure 3 displays the boost type converter's basic circuit design.

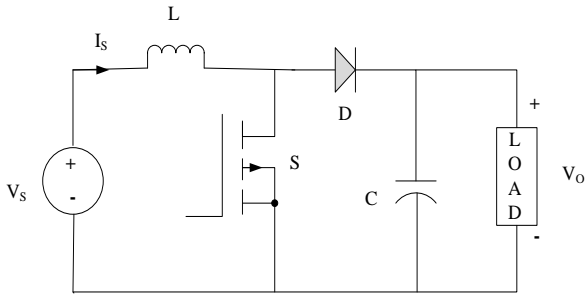


**Fig 3:** Circuit diagram of DC-to-DC converter

In this above circuit diagram the input source is connected to inductor for constant output and there is a switch (FET) in which the diode is connected to capacitor. The load connected in it is constant voltage source and this voltage is obtained by frequency modulation. The two modes of operation is given below [23; 24],

- Switch is ON , diode is OFF
- Switch is OFF, diode is ON

The second mode is choosing for getting more output current and the steady state equation for second mode is given in equation (8-10),

$$V_{in} = V_L + V_O \quad (8)$$

$V_{in}$  is output voltage from PV panel, the inductor's voltage across it is  $V_L$  and converter's output voltage is  $V_O$ .

$$V_L = L \frac{di_L}{dt} = V_{in} - V_O \quad (9)$$

$$\frac{di_L}{dt} = \frac{\Delta i_L}{\Delta t} = \frac{\Delta i_L}{(1-D)T} = \frac{V_{in} - V_O}{L} \quad (10)$$

$D$  stands for duty cycle. Since the switch is in the open position for the duration specified in equation (11)

$$T_{OFF} = T - T_{ON} = T - DT = (1-D)T$$

We can say that  $\Delta t = (1-D)T$

$$\Delta i_L (open) = \frac{V_{in} - V_O}{L} * (1-D)T \quad (11)$$

Output voltage is solved from below equations (12-15)

$$\therefore \Delta i_L (open) + \Delta i_L (close) = 0 \quad (12)$$

$$\frac{V_{in} - V_O}{L} * (1-D)T + \left( \frac{-V_O}{L} * DT \right) = 0 \quad (13)$$

$$\frac{V_O}{V_{in}} = \frac{1}{1-D} \quad (14)$$

$$\therefore V_O = \frac{1}{1-D} * V_{in} \quad (15)$$

#### 4.2. HBA based algorithm for maximum power generation

The algorithm known as HBA, which is based on the feeding habits of honey badgers, should be used to optimize the electricity produced by PV panels. It locates the prey by digging and smelling, otherwise it directly approaches the beehive by following the honey guide bird. In a single day, it may dig fifty holes with a 40-kilometer radius. There are two stages to this algorithm: the honey phase and the digging phase. Each step of this algorithm is explained below [25]. This algorithm shows in figure 4 is based on exploration and exploitation phase and the population candidate solution is given in equation (16)

Population candidate solution=

$$\begin{bmatrix} x_{11} & x_{12} & \dots & x_{1D} \\ x_{21} & x_{22} & \dots & x_{2D} \\ \dots & \dots & \dots & \dots \\ x_{n1} & x_{n2} & \dots & x_{nD} \end{bmatrix} \quad (16)$$

Honey badger is in the position of  $i$  which is expressed in equation (17),

$$x_i = x_i^1 + x_i^2 + \dots + x_i^D \quad (17)$$

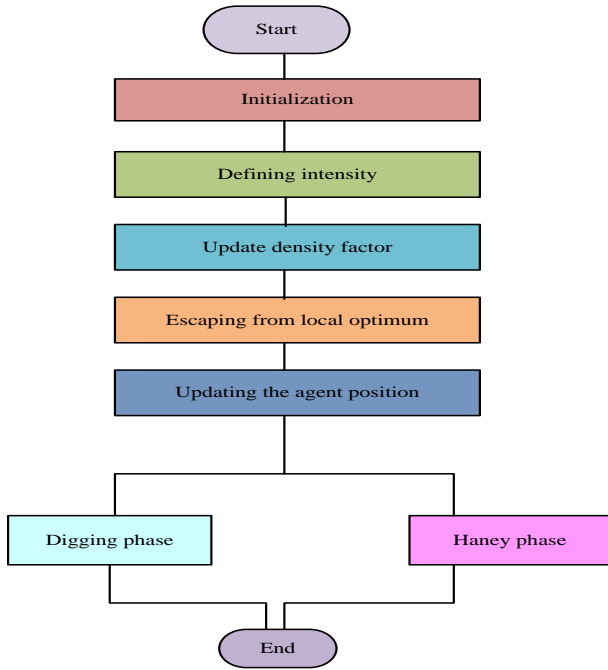


**Fig 4:** Flow chart of HBA algorithm

The geographic distribution and population number ( $N$ ) of honey badgers at the beginning phase are given by equation (18).

$$x_i = lb_i + r_1 \times (ub_i - lb_i) \quad (18)$$

Here,  $lb_i$  and  $ub_i$  represent the lower and higher values of the search domain, and  $r$  is a random number between 0 and 1.

The level of focus and the separation between the honey badger's target and its prey at that particular spot dictate how intense a hunt will be. Here  $I_i$  is the smell intensity and if the smell intensity increases the speed will also increase which is expressed as inverse square law in equation (19-21)

$$I_i = r_2 \times \left( \frac{S}{4\pi d_i^2} \right) \quad (19)$$

$$S = (x_i - x_{i+1})^2 \quad (20)$$

$$d_i = x_{prey} - x_i \quad (21)$$

Here, Prey's concentration intensity is denoted by  $S$ ; conversely,  $d_i$  represents the distance between the  $i^{th}$  badger and the prey. Density factor ( $\alpha$ ) makes smooth transition by controlling time-varying randomization from exploration to exploitation. For decreasing the iteration with time, update  $\alpha$  which is given in equation (22).

$$\alpha = C \times \exp\left(\frac{-t}{t_{max}}\right) \quad (22)$$

Here,  $C$  is the constant that is higher than or equal to the value 1 (default=2), and  $t_{max}$  is the maximum number of repetitions.

Here, the suggested method switches the search orientation by using a flag  $F$ , as seen in Figure 5, in order to obtain high, which is then utilized to scan the search space in order to escape from local optima [26].

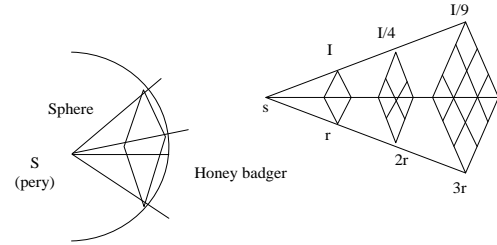


**Fig 5:** Search direction of honey badger

There are two stages to the updating process ( $x_{new}$ ): the digging phase and the honey phase. As explained above. Movement of the honey badger resembles cardioids, and equation (23), which describes this motion, represents the cardioids motion.

$$x_{new} = x_{prey} + F \times \beta \times I \times x_{prey} + F \times r_3 \times \alpha \times d_i \times |\cos(2\pi r_4)| \times [1 - \cos(2\pi r_5)] \quad (23)$$

where  $\beta$  is higher than or equal to 1 (default = 6),  $x_{prey}$  is the position of the prey that fits the profile the best,  $d_i$  is the distance between the prey and the  $i^{th}$  honey badger, and  $r_3$ ,  $r_4$ , and  $r_5$  are three distinct random integers between 0. Value of  $F$  is expressed in equation (24)

$$F = \begin{cases} 1 & \text{if } r_6 \leq 0.5 \\ -1 & \text{else} \end{cases} \quad (24)$$

Here, The random number,  $r_6$ , ranges from 0 to 1. Moreover, in digging phase, any disturbance  $F$  received by badger is used to find better prey location. The honey phase is expressed in equation (25) below, which clarifies the honey badger's behavior in accompanying the beehive's honey bird.

$$x_{new} = x_{prey} + F \times r_7 \times \alpha \times d_i \quad (25)$$

At the moment, time-varying search behavior ( $\alpha$ ) influences the lookup. In addition, a honey badger may find disruption  $F$ .

### 4.3. Performance and circuit diagram of DC to AC inverter

Output of maximum power from DC-DC converters is given to the input of DC-AC inverter in which multilevel inverter (cascaded H-Bridge (CHB) is

used. Figure 6 shows the circuit diagram of CHB inverter [27].

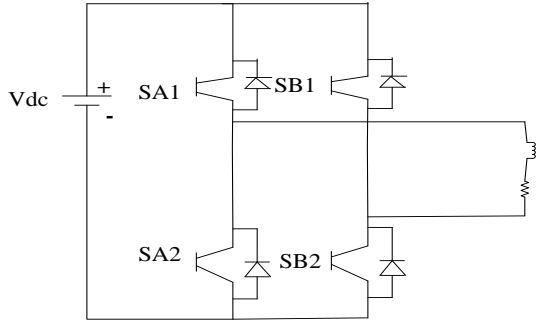


**Fig 6:** Circuit diagram of DC-AC converters

Figure 6 above shows the configuration of two or more H-bridge inverters powered by a single DC source from the CHB. This kind of inverter uses four power electronic switches since it is a single-cell H-bridge inverter. Every inverter cell may use the same modulation mechanism or a different one. It can be either of the following: carrier-based PWM, fundamental switching frequency PWM, or a hybrid or mixed PWM approach that combines the two. This circuit's output is supplied to loads and the grid [28].

#### 4.4. COA based stability enhancement optimization

The suggested method analyzes the PV panel arrangement and maintains system efficiency through the use of a recently developed optimization technique termed COA. Its core concept is derived from species of cane latrines found in North America. The social structure of the coyote agents is defined by modifying the algorithm. Main benefit of this approach is that it maintains equilibrium between the mechanisms of exploration and exploitation throughout the optimization process. Figure 7's flow chart explains the algorithm's operation.

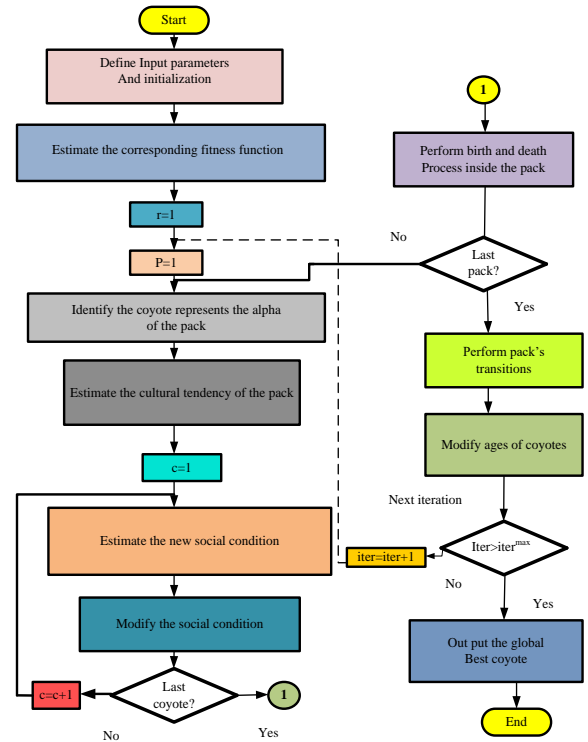


**Fig 7:** Flow chart of COA algorithm

COA is dependent on the coyotes' social structure and routine experience exchange, in addition to their hunting prey [29]. As they move in a close chain toward the prey, their cooperative functions set them apart. Considering that they have an acute sense of smell, they can locate their prey. Coyotes attack in packs, which compels them to adjust and strengthen their positions. Coyotes migrate a great deal of random distance from their current locations, well-prepared with a chance of threat, when they strike their opponents. Equation (26) defines the coyote's social behavior, which is used as a collection of design factors.

$$SOC_c^{p,t} = \vec{x} = (x_1, x_2, x_3, \dots, x_D) \quad (26)$$

The coyote must adjust to the surroundings due to this social situation, which is known as  $fit_c^{p,t} \in \mathfrak{R}$ .

Equation (27) provides an assessment of the coyotes' adaptability to their existing social conditions.

$$fit_c^{p,t} = f(SOC_c^{p,t}) \quad (27)$$

Initially the coyotes are in random packs after sometime it will move and change their packs. Coyotes move between packs, enhancing their engagement to a significant degree are shown in alpha which is given in equation (28).

$$alpha = \left\{ SOC_c^{p,t} \left| \arg \min_{c=\{1,2,\dots,N_c\}} f(SOC_c^{p,t}) \right. \right\} \quad (28)$$

Cultural tendency is defined as the existing information shared by coyotes when all coyotes are arranged and exchange in social culture which is given in equation (29, 30),

$$cult_j^{p,t} = \begin{cases} O_{\left(\frac{N_c+1}{2}\right)}^{p,t} & ; N_c \text{ is odd} \\ \frac{O_{\frac{N_c}{2}}^{p,t} + O_{\left(\frac{N_c+1}{2}\right)j}^{p,t}}{2} & ; otherwise \end{cases} \quad (29)$$

Where  $O^{p,t}$  is a rating of the general social state of all coyotes at any given time, a pack's cultural predisposition is determined by the average social circumstances among every coyote inside that pack. In this  $age_c^{p,t}$  is the birth of new coyotes, this, as a consequence of the pair of parents' social combination selecting at random, is represented by equation (30),

$$pup_j^{p,t} = \begin{cases} SOC_{r1,j}^{p,t} & ; rnd \alpha P_s \text{ or } j = j_1 \\ \frac{SOC_{r2,j}^{p,t}}{2} & ; rnd \alpha P_s + P_a \text{ or } j = j_2 \\ R_j & ; otherwise \end{cases} \quad (30)$$

where,  $SOC_{r1,j}^{p,t}$  is the Social conditions of coyote r1,  $SOC_{r2,j}^{p,t}$  is the Social condition of coyote r2, The optimization problem's dimensions are  $j_1, j_2$ , the number in the range of variables boundaries is  $R_j$ , and the probabilities of scatter and association are  $P_a$  and  $P_s$ .

Computation of coyote cultural diversity is based on  $P_a$  and  $P_s$  from pack which is given below,

$$P_s = \frac{1}{D}, P_a = \frac{1 - P_s}{D}$$

For simulation we have to consider two parameters. These are the worst pack effect  $\delta$  and fitness function  $w$ , where the number of coyotes in the group is represented by  $Q$ . Equation (31, 32) mentions this function.

$$\delta = \alpha^{p,t} - SOC_{cr2}^{p,t} \quad (31)$$

$$\delta = cult^{p,t} - SOC_{cr2}^{p,t} \quad (32)$$

The alpha and pack effect is important while updating coyotes which is shown in equation (33),

$$SOC_c^{p,t,new} = SOC_c^{p,t,old} + r1.\delta1 + r2.\delta2 \quad (33)$$

Reports on the condition of society of coyotes are given below equation (34),

$$SOC_c^{p,t+1} = \begin{cases} SOC_c^{p,t,new} \cdot fit_c^{p,t} \cdot \alpha fit_c^{p,t} \\ SOC_c^{p,t} \cdot otherwise \end{cases} \quad (34)$$

Thus the output is maintained efficiently and accurately by using the above mentioned optimization technique. The effectiveness of maximum power generation progress is confirmed using the system's simulated output, as explained in more detail in the section that follows.

## 5. Results and Discussion

The simulation circuit and waveforms for the suggested method are displayed below after it has been simulated using the MATLAB software. In comparison to other current techniques, the MPPT controller in this part tracks the highest power at the least amount of time using the HBA methodology, which provides high efficiency. The MPPT controller, inverter, DC-DC converter, and PV panel comprise the simulated circuit for the project. PV panels with different irradiance levels are the input of the proposed system. In this proposed system the tracking efficiency is improved by using proposed technique is used in MPPT controller for tracking most force in the shortest amount of time. The following result shows the load, converter output voltage, and PV panel output power. Plotting of system constraints, parameter determination, and data presentation are provided in Table 1. Boundaries such as voltage, current, and power are utilized to evaluate both normal and abnormal situations. The testing technique requires a simulation time of 0–5 s.

**Table.1:** Implementation parameters

Parameters	Values
<b>PV</b>	
Maximum Power (W)	9kW
Cells per module (Ncell)	96
Open circuit voltage Voc (V)	64.2
Short-circuit current Isc (A)	5.96
Voltage at maximum power point Vmp (V)	54.7
Current at maximum power point Imp (A)	5.58
Light-generated current IL (A)	6.0092
Diode saturation current I0 (A)	6.30e-12
Diode ideality factor	0.94504
Shunt resistance Rsh (ohms)	269.5934
Series resistance Rs (ohms)	0.37152
<b>Three phase Filter</b>	
Nominal phase-to-phase voltage Vn (Vrms)	260
Nominal frequency fn (Hz)	60

**Table 2:** Simulation result for tracking time and efficiency

Optimization Technique	Tracking time in sec			Tracking Efficiency (%)
	Irradiance = 1000 (W/m <sup>2</sup> ) P <sub>mpp</sub> = 2490.75 W	Irradiance = 900 (W/m <sup>2</sup> ) P <sub>mpp</sub> = 2235.4 W	Irradiance = 700 (W/m <sup>2</sup> ) P <sub>mpp</sub> = 1728.23 W	
IPSO	8.20	8.01	7.92	85.73
GWO	4.26	3.77	4.15	95.86
IP&O	3.65	3.15	2.87	99.38
Proposed	1.25	1.53	1.55	99.49

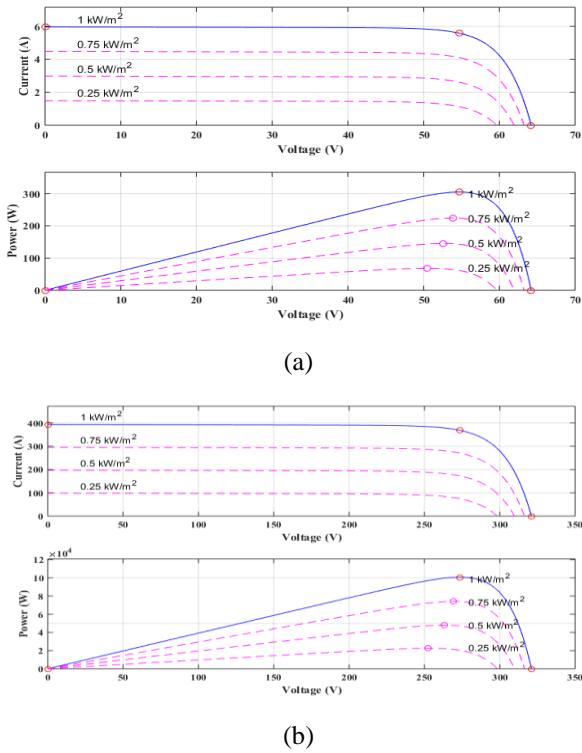


**Fig 8:** IV and PV characteristics of (a) module and (b) array

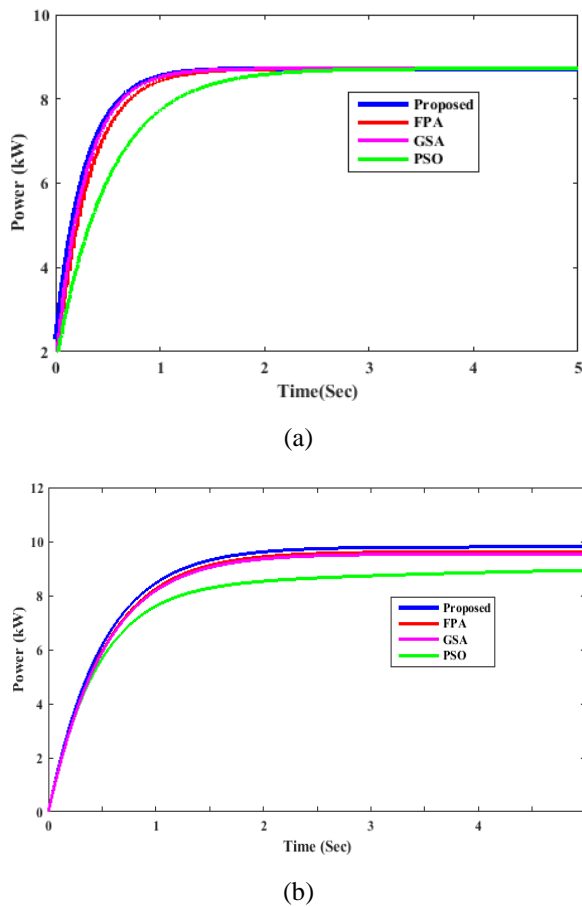


**Fig.9:** Comparison Analysis of different partial shading conditions

Figure 8 shows the PV characteristics, which also include PV module and array characteristics as well as P-V and I-V attributes. A DC-DC converter that utilizes the HBA algorithm promotes maximum power generation. The resulting power comparison evaluations between the recommended strategy and other approaches that are currently in use are displayed in Figure 9. Table 2 describes the tracking efficiencies and the induced power. Furthermore, the three-phase filter and the VSI were used to send the generated energy to the grid. The correctness and efficacy of the system are demonstrated by the comparison study of the suggested technique. It is possible to compare the DC connection voltage and power produced by the recommended technique and the existing approaches. The analysis concludes that the suggested approach for managing power yields better outcomes between the grid side and the generating side. A detailed study of the suggested technique's efficacy is provided based on the comparison analysis. The suggested method's comparative analysis has been effectively examined and validated.

## 6. Conclusion

In the stand-alone power system, the MPPT controller for solar power generation uses a new tracking technique for HBA that is proposed in this study. The MPPT controller uses an HBA approach to make the most out of the power generation that is available. The benefits of the HBA approach include a reduced computing load and a faster, more dependable searching capability. This allows the MPPT to operate on the PV panel in any weather conditions. Since the suggested tracking methodology has been shown to monitor most power in the shortest amount of time, the efficiency of the tracking system is higher than that of other methods. Furthermore,

a comparison is made between the suggested MPPT methodology and the existing methods. The system performance is verified once the hardware configuration is in place and information is obtained from the solar emulator for the output signals PPV, IPV, and VPV.

#### **Declaration Of Interests:**

#### **Funding**

On Behalf of all authors the corresponding author states that they did not receive any funds for this project.

#### **Conflicts Of Interest**

The authors declare that we have no conflict of interest.

#### **Competing Interests**

The authors declare that we have no competing interest.

#### **Data Availability Statement**

All the data is collected from the simulation reports of the software and tools used by the authors. Authors are working on implementing the same using real world data with appropriate permissions.

#### **Ethics Approval**

No ethics approval is required.

#### **Consent To Participate**

Not Applicable

#### **Consent For Publication**

Not Applicable

#### **References**

- [1] Joe-Air Jiang, Yu-Li Su, Jyh-Cherng Shieh, Kun-Chang Kuo, Tzu-Shiang Lin, Ta-Te Lin, Wei Fang., Jui-Jen Chou, Jen- Cheng Wang, "On application of a new hybrid maximum power point tracking (MPPT) based photovoltaic system to the closed plant factory," *Applied Energy*, vol. 124, pp. 309- 324, April 2014.
- [2] Hadeed Ahmed Sher, Ali Faisal Murtaza, Abdullah Noman, Khaled E. Addoweesh, Kamal Al-Haddad and Marcello Chiaberge, "A New Sensor less Hybrid MPPT Algorithm Based on Fractional Short-Circuit Current Measurement and P&O MPPT," *IEEE Transactions on Sustainable Energy*, Vol. 6, No. 4, Pp. 1426-1434, 2015
- [3] S.M.Reza Tousi, Mohammad Hassan Moradi, Nasser Saadat Basir and Milad Nemati, "A Function-Based Maximum Power Point Tracking Method for Photovoltaic Systems," *IEEE Transactions on Power Electronics*, Vol. 31, No. 3, Pp. 2120-2128, 2016
- [4] Antonio Alisson Alencar Freitas, Fernando Lessa Tofoli, Edilson Mineiro Sa Junior, Sergio Daher and Fernando Luiz Marcelo Antunes, "High-voltage gain dc-dc boost converter with coupled inductors for photovoltaic systems," *IET Power Electronics*, Vol. 8, No. 10, Pp. 1885-1892, 2015
- [5] Dinesh K Sharma and Ghanshyam Purohit, "Differential power algorithm based maximum power point tracking for a standalone solar PV system," *Energy in Southern Africa*. Vol. 26, No. 2, 2015
- [6] Shiqing Tang, Yize Sun, Yujie Chen, Yiman Zhao, Yunhu Yang and Warren Szeto, "An Enhanced MPPT Method Combining Fractional-Order and Fuzzy Logic Control," *IEEE Journal of Photovoltaics*, Vol. 7, No. 2, 2017
- [7] Yie-Tone Chen, Zhi-Hao Lai and Ruey-Hsun Liang, "A novel auto-scaling variable step-size MPPT method for a PV system," *Solar Energy*, Vol. 102, Pp. 247-256, 2014
- [8] Jia Liu, Rui Tian and Jing Nie, "Effect of impeller solidity on the generating performance for solar power generation", *Journal of Electronic Science and Technology*, Vol. 19, No. 100132, 2021
- [9] N.Prabaharan and K. Palanisamy, "Analysis and integration of multilevel inverter configuration with boost converters in a photovoltaic system," *Energy Conversion and Management*, Vol. 128, Pp. 327-342, 2016
- [10] Ali Moghassemi, Shayan Ebrahimi, Sanjeevikumar Padmanaban, Massimo Mitolo and Jens Bo Holm-Nielsen, "Two fast metaheuristic-based MPPT techniques for partially shaded photovoltaic system", *International Journal of Electrical Power & Energy Systems*, Vol. 137, No. 107567, 2022
- [11] Resat Celikel, Musa Yilmaz, Ahmet Gundogdu, "A voltage scanning-based MPPT method for PV power systems under complex partial shading conditions", *Renewable Energy*, Vol. 184, Pp.361-373, 2022
- [12] Akhil Raj, Sabha Raj Arya, Jyoti Gupta, "Solar PV array-based DC-DC converter with MPPT for low power applications", *Renewable Energy Focus*", Vol. 34,Pp. 109-119, 2020
- [13] A.Attou, A.Massoum and M.Saidi, "Photovoltaic Power Control Using MPPT and Boost Converter," *Balkan Journal of Electrical & Computer Engineering*, Vol. 2, No. 1, 2014
- [14] Yaduvir Singh, Nitai Pal, "Reinforcement learning with fuzzified reward approach for MPPT control

- of PV systems", *ustainable Energy Technologies and Assessments*, Vol. 48, No. 101665, 2021
- [15] Akhil Raj, Sabha Raj Arya and Jyoti Gupta, "Solar PV array-based DC–DC converter with MPPT for low power applications", *Research Paper*, Vol. 34, Pp. 109-119, 2020
- [16] M.Lakshmi and S.Hemamalini, "Coordinated control of MPPT and voltage regulation using single-stage high gain DC–DC converter in a grid-connected PV system", *Electric Power Systems Research*, Vol. 169, Pp. 65-73, 2019
- [17] Khaled Osmani, Ahmad Haddada, Thierry Lemenand, Bruno Castanier and Mohamad Ramadana, "An investigation on maximum power extraction algorithms from PV systems with corresponding DC-DC converters", *Energy*, Vol. 224, No. 120092, 2021
- [18] Armando Cordeiro, V.Fernao Pires, Daniel Foito, A.J.Pires and J.F.Martins, "Three-level quadratic boost DC-DC converter associated to a SRM drive for water pumping photovoltaic powered systems", *Solar Energy*, Vol. 209, Pp. 42-56, 2020
- [19] Ahmed T.Mohamed, Mahmoud F.Mahmoud, R.A.Swief, Lobna A.Said and Ahmed G.Radwan, "Optimal fractional-order PI with DC-DC converter and PV system", *Ain Shams Engineering Journal*, Vol. 12, No. 2, Pp. 1895-1906, 2021
- [20] S.M.Sousa, L.S.Gusman, T.A.S.Lopes, H.A.Pereira and J.M.S.Callegari, "MPPT algorithm in single loop current-mode control applied to dc–dc converters with input current source characteristics", *International Journal of Electrical Power & Energy Systems*, Vol. 138, No. 107909, 2022
- [21] Fengyuan Wang, Shuai Zhang, Chenyu Lv, Linlin Liu, Yu Zhuang, Lei Zhang and Jian Du, "Optimal design of solar-assisted steam and power system under uncertainty", *Journal of Cleaner Production*, Vol. 336, No. 130294, 2022
- [22] Fatih Bayrak, Hakan F.Oztop and Fatih Selimefendigil, "Experimental study for the application of different cooling techniques in photovoltaic (PV) panels", *Energy Conversion and Management*, Vol. 212, No. 112789, 2020
- [23] G.Kanimozhi, J.Meenakshi and V.T.Sreedevi, "Small Signal Modeling of a DC-DC Type Double Boost Converter Integrated With SEPIC Converter Using State Space Averaging Approach", *Energy Procedia*, Vol. 117, Pp. 835-846, 2017
- [24] Qingyu Su, Chenglong Li, Xinxin Guo, Xinquan Zhang and Jian Li, "Robust fault diagnosis for DC–DC Boost converters via switched systems", *Control Engineering Practice*, Vol. 112, No. 104836, 2021
- [25] Fatma A.Hashim, Essam H.Houssein, Kashif Hussain, Mai S.Mabrouk AND Walid Al-Atabany, "Honey Badger Algorithm: New metaheuristic algorithm for solving optimization problems", *Mathematics and Computers in Simulation*, Vol. 192, Pp. 84-110, 2022
- [26] Erfeng Han and Noradin Ghadimi, "Model identification of proton-exchange membrane fuel cells based on a hybrid convolutional neural network and extreme learning machine optimized by improved honey badger algorithm", *Sustainable Energy Technologies and Assessments*, Vol. 52, No. 102005, 2022
- [27] D.Arun Prasad, K.Mahadevan and M.Arul Prasanna, "A modified asymmetric cascaded multilevel DC–AC converter with switched diodes using FPGA processor implementation", *Microprocessors and Microsystems*, Vol. 74, No. 103019, 2020
- [28] Nibedita Parida and Anandarup Das, "A New Modular Multilevel Converter Circuit Topology with Reduced Number of Power Cells for DC to AC Applications", *International Journal of Electrical Power & Energy Systems*, Vol. 123, No. 106256, 2020
- [29] Varaprasad Janamala and D Sreenivasulu Reddy, "Coyote optimization algorithm for optimal allocation of interline –Photovoltaic battery storage system in islanded electrical distribution network considering EV load penetration", *Journal of Energy Storage*, Vol. 41, No. 102981, 2021